TECHNICAL NOTE

D-1534

A NUMERICAL SOLUTION OF THE PROBLEM OF MIXING OF LAMINAR COAXIAL STREAMS OF GREATLY DIFFERENT DENSITIES - ISOTHERMAL CASE

By Herbert Weinstein and Carroll A. Todd

Lewis Research Center
Cleveland, Ohio

NATIONAL AERONAUTICS AND SPACE ADMINISTRATION

WASHINGTON

February 1963

Code -1

SINGLE COPY ONLY

NATIONAL AERONAUTICS AND SPACE ADMINISTRATION

TECHNICAL NOTE D-1534

A NUMERICAL SOLUTION OF THE PROBLEM OF MIXING OF LAMINAR COAXIAL STREAMS OF GREATLY DIFFERENT DENSITIES - ISOTHERMAL CASE

By Herbert Weinstein and Carroll A. Todd

SUMMARY

The system under consideration is a slow-moving, heavy inner stream surrounded by a fast-moving, light outer stream infinite in extent. The flow region of interest lies between the inner jet entrance and the end of the potential core. The density ratio of the two streams may vary through several orders of magnitude, and no restrictions are placed on the velocities of the two components. The only information required is the initial velocity and concentration profiles and the physical properties of the fluids.

An equation set is derived and solved numerically for several sets of input parameters. A system of equations that is not extremely sensitive to physical property variations results from the manner in which the variables are made dimensionless. A diffusion equation valid for high values of the density ratio is employed. No consideration is given to the hydrodynamic stability of the system.

Results are calculated for a given set of physical properties and a range of values of density and velocity ratio. These results include:

1. The potential core length is approximately 6 radii for fluids of the same density and a velocity ratio of 100.

2. For values of density ratio above 20, the effect of varying density ratio is small.

3. For Froude numbers of 10^2 or less, the mass and momentum transfer become second-order effects compared to the acceleration due to the force field.

4. Large changes in the values of physical properties of the two fluids cause relatively small changes in potential core length.

INTRODUCTION

There has been considerable discussion in recent years on the mixing of laminar coaxial streams of different densities (refs. 1 and 2). However, the density ratios of the two streams considered have almost always been approximately 2 or less. The coaxial-flow, gaseous-reactor concept developed in the recent past (ref. 3) and the work on coaxial streams of plasma and coolant (ref. 4) have spurred interest in the coaxial flow of gases with density ratios of 5 to 100.

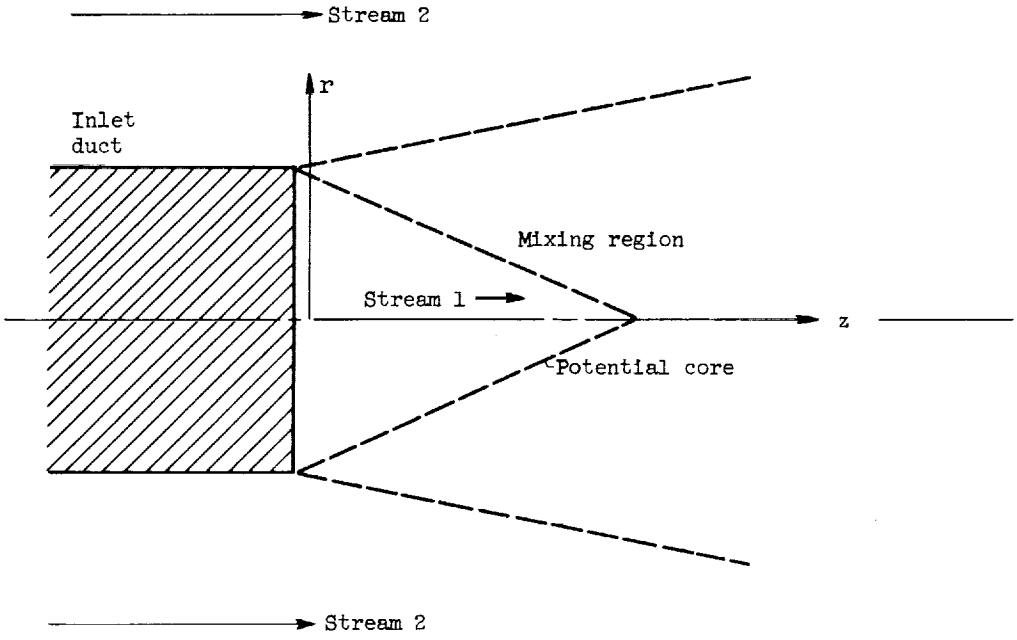

Figure 1. - Flow system.

The system considered here and shown in figure 1 is that of a slow-moving, heavy inner stream surrounded by a fast-moving light outer stream infinite in extent. The flow region of interest is that between the inner jet entrance and the end of the potential core. This potential core is defined as the relatively undisturbed inner stream fluid. The ratio of the densities of the two streams may vary through several orders of magnitude; as long as the flow is laminar, there are no limits on the velocities of the two components. The initial velocity and concentration profiles and the physical properties of the fluids are the only information that is required. Any initial velocity profile may be specified.

The hydrodynamic equations are transformed to a stream-function coordinate set and then integrated numerically from the initial conditions. No attempt was made to uncouple the simultaneous differential equations as this has always forced restrictions on the density variation. It was felt that, in order to maintain a reasonable degree of accuracy in the solution, it would be best to

the burden of the computations on the digital computer. The method of attack used here is similar to that of Pai (ref. 1), but it is concerned with a cylindrical geometry whereas Pai's work is for a Cartesian system. The diffusion equation used by Pai limits his work to density ratios of about 1 or 2, while this work employs a diffusion equation that is also correct for much higher values of density ratio. The manner in which the variables are made dimensionless is different from that of Pai and results in a system of equations that are not very sensitive to physical property variations. Velocity ratios instead of velocity differences are considered when the system is being defined.

The quantities of major interest calculated and presented here are the length of potential core, the average axial velocity of the inner fluid, and the inner-fluid average density for various values of initial density ratio and initial velocity ratio of the two streams. Sample velocity and concentration profiles are also shown to illustrate the changes in the profiles with increasing axial distance downstream. Cases with both flat and parabolic initial velocity profiles are presented to indicate the effect the shape of the initial velocity profile has on potential core length. The effect of a body force directed along the axis of the flow system is shown because this effect would be present in a coaxial-flow, gaseous-reactor concept. Finally, the values of the parameters (i.e., Schmidt number, Reynolds number, viscosity ratio, and diffusion coefficient) are varied to demonstrate their effect on the aforementioned values.

Presented here, then, are the results of an accurate numerical solution of a laminar, isothermal coaxial-flow system in which the two fluids have greatly different densities. The method is similar to that of Pai but differs on several important points. No consideration has been given to the hydrodynamic stability of the system.

SYMBOLS

a acceleration due to body force

C concentration (mole fraction) of inner-stream component

D diffusivity

F Froude number

K Boltzmann constant

L length

m molecular weight

N molar density of fluid

P pressure

Re	Reynolds number
r	radial length variable
Sc	Schmidt number
T	temperature
u	axial velocity component
V	molecular volume
v	radial velocity component
z	axial length variable
β	$(m_1/m_2) - 1$
ϵ	maximum energy of attraction for Lennard-Jones potential
μ	viscosity
ρ	mass density
σ	molecular diameter
ψ	stream function
Ω	arithmetic mean molecular speed

Subscripts:

av	average value for all r positions at a given z
L	length
max	maximum
0	initial conditions
1	inner stream
2	outer stream
11	self diffusion
12	binary diffusion

Superscript:

$(\bar{\ })$ dimensionless variable

ANALYSIS

The derivation of the equation set that describes the coaxial-flow system is presented here. The numerical methods employed in the solution of these equations are described in appendix A.

Assumptions and Restrictions

The assumptions and restrictions made in deriving the equation set are listed here, not necessarily in order of importance:

(1) The entire flow field is at a constant temperature.

(2) The entire flow field is at a constant pressure.

(3) There is axial symmetry in the flow system.

(4) The fluids mix ideally; there is no pressure, temperature, or volume change on mixing.

(5) There is steady state in the system.

(6) The normal boundary-layer assumptions are used; that is,

$$\frac{\partial u}{\partial r} \gg \frac{\partial u}{\partial z},\ u \gg v,\ \frac{\partial C}{\partial r} \gg \frac{\partial C}{\partial z},\ \ldots$$

(7) The assumption $\partial\psi/\partial r \gg \partial\psi/\partial z$, which follows from $u \gg v$, is stated separately because it is used again in a transformation of coordinates.

Derivation of Equation Set

The continuity, momentum, and diffusion equations are given for the system shown in figure 1 (eqs. (1), (2), and (3)). The continuity equation already contains the steady-state and axisymmetric assumptions. The momentum equation is the result of simplifying the Navier-Stokes equation with the steady-state, constant-pressure, axisymmetric, and boundary-layer assumptions. The last term of this equation, which includes the effect of the buoyancy of the outer stream, describes the effect of a body force directed along the axis and away from the entrance. The diffusion equation (ref. 5), which contains the steady-state and axisymmetric assumptions but no assumptions as to the variation in density, is correct for large density variations. No pressure or thermal diffusion is considered here as noted by assumptions (1) and (2) of the aforementioned list.

Each equation is written for variable density and applies over the whole flow field because the gases form a continuum. Only density changes that are caused by mixing are considered.

Continuity:

$$\frac{\partial}{\partial r}(\rho v r) + \frac{\partial}{\partial z}(\rho u r) = 0 \tag{1}$$

Momentum:

$$v\frac{\partial u}{\partial r} + u\frac{\partial u}{\partial z} = \frac{1}{\rho r}\frac{\partial}{\partial r}\left(r\mu\frac{\partial u}{\partial r}\right) + \frac{a(\rho - \rho_2)}{\rho} \tag{2}$$

Diffusion:

$$v\frac{\partial C}{\partial r} + u\frac{\partial C}{\partial z} = \frac{\rho}{r}\frac{\partial}{\partial r}\left(\frac{rD_{12}}{\rho}\frac{\partial C}{\partial r}\right) \tag{3}$$

Since the fluids mix ideally, the density at a point is equal to the sum of the partial densities at that point. Since the temperature and pressure are constant, the molar density N is constant and the mass density ρ can be expressed as

$$\rho = m_2 N\left[\left(\frac{m_1}{m_2} - 1\right)C + 1\right]$$

This can be expressed with the definition

$$\beta = \frac{m_1}{m_2} - 1$$

as

$$\rho = m_2 N(\beta C + 1) \tag{4}$$

Introducing the dimensionless quantities

$$\bar{D} = \frac{D_{12}}{D_{11}} \qquad \bar{r} = \frac{r}{r_0} \qquad \bar{u} = \frac{u}{u_{1,0}}$$

$$\bar{z} = \frac{z}{r_0} \qquad F = \frac{u_{1,0}^2}{r_0 a} \qquad \bar{v} = \frac{v}{u_{1,0}}$$

$$\bar{\mu} = \frac{\mu}{\mu_1} \qquad Re_{1,0} = \frac{r_0 u_{1,0}\rho_{1,0}}{\mu_{1,0}} \qquad Sc_{1,0} = \frac{\mu_{1,0}}{\rho_{1,0}D_{11}}$$

and substituting these and equation (4) into equations (1) to (3) result in the following dimensionless equations:

Continuity:

$$\frac{\partial}{\partial r}\left[\overline{rv}(\beta C + 1)\right] + \frac{\partial}{\partial z}\left[\overline{ru}(\beta C + 1)\right] = 0 \tag{5}$$

Momentum:

$$\bar{v}\frac{\partial \bar{u}}{\partial r} + \bar{u}\frac{\partial \bar{u}}{\partial z} = \frac{1}{Re_{1,0}}\frac{\beta + 1}{\beta C + 1}\frac{1}{\bar{r}}\frac{\partial}{\partial r}\left(\overline{\mu r}\frac{\partial \bar{u}}{\partial r}\right) + \frac{\beta C}{\overline{F(\beta C + 1)}} \tag{6}$$

Diffusion:

$$\bar{v}\frac{\partial C}{\partial r} + \bar{u}\frac{\partial C}{\partial z} = \frac{1}{Re_{1,0}Sc_{1,0}}\frac{\beta C + 1}{\bar{r}}\frac{\partial}{\partial r}\left(\frac{\overline{Dr}}{\beta C + 1}\frac{\partial C}{\partial r}\right) \tag{7}$$

The stream function ψ is defined by the following relations:

$$\left.\begin{aligned}\frac{\partial \psi}{\partial z} &= -\frac{1}{\overline{rv}}(\beta C + 1)\\ \frac{\partial \psi}{\partial r} &= \frac{1}{\overline{ru}}(\beta C + 1)\end{aligned}\right\} \tag{8}$$

This satisfies the dimensionless continuity equation.

The dimensionless transport properties $\bar{D}$ and $\bar{\mu}$ are evaluated from the ratio of the values of the pure components and also in the case of viscosity from an elementary mixing equation. The mixing equation used for viscosity is

$$\mu = \frac{m}{\frac{Cm_1}{\mu_{1,0}} + \frac{(1 - C)m_2}{\mu_{2,0}}}$$

(ref. 6), which upon substitution of the dimensionless groups, reduces to

$$\bar{\mu} = \frac{\beta C + 1}{(\beta + 1)C + \frac{1 - C}{\frac{\mu_{2,0}}{\mu_{1,0}}}} \tag{9}$$

The dimensionless diffusivity is calculated from the Gilliland equation in the following manner:

$$\overline{D} = \frac{D_{12}}{D_{11}} = \frac{2V_1^{1/3}}{V_1^{1/3} + V_2^{1/3}} \sqrt{\frac{m_1}{2}\left(\frac{1}{m_1} + \frac{1}{m_2}\right)}$$

Introducing $\overline{V}_2 = V_2/V_1$ results in

$$\overline{D} = \frac{\sqrt{2(\beta + 2)}}{1 + \overline{V}_2^{1/3}} \tag{10}$$

The dimensionless diffusivity can also be derived in a somewhat different but equivalent form from a Lennard-Jones potential argument. This method was not used, but it is presented in appendix B by way of illustration. The more rigorous Lennard-Jones potential argument provides an alternate constant value for $\overline{D}$.

The momentum diffusion and energy equations are now transformed to the $z - \psi$ plane in the following manner. Originally, ψ, C, and $\overline{u}$ are functions of the spatial coordinates as follows:

$$\psi = \psi(\overline{r},\overline{z})$$

$$C = C(\overline{r},\overline{z})$$

$$\overline{u} = \overline{u}(\overline{r},\overline{z})$$

and after the transformation functional relations of C, $\overline{u}$, and the spatial coordinate $\overline{r}$ in terms of ψ and the spatial coordinate $\overline{z}$ are obtained:

$$\overline{r} = \overline{r}(\psi,\overline{z})$$

$$C = C(\psi,\overline{z})$$

$$\overline{u} = \overline{u}(\psi,\overline{z})$$

The relations for the transformations are

$$\left.\begin{aligned}\left(\frac{\partial}{\partial \overline{z}}\right)_r &= \left(\frac{\partial}{\partial \overline{z}}\right)_\psi + \left(\frac{\partial \psi}{\partial \overline{z}}\right)_r \left(\frac{\partial}{\partial \psi}\right)_z \\ \left(\frac{\partial}{\partial \overline{r}}\right)_z &= \left(\frac{\partial \psi}{\partial \overline{r}}\right)_z \left(\frac{\partial}{\partial \psi}\right)_z\end{aligned}\right\} \tag{11}$$

Transforming the momentum and diffusion equations (eqs. (6) and (7)) with equation (10) produces the following:

Momentum:

$$\frac{\partial \bar{u}}{\partial \bar{z}} = \frac{\beta + 1}{Re_{1,0}} \frac{\partial}{\partial \psi} \left[\overline{\mu r^2} \bar{u} (\beta C + 1) \frac{\partial \bar{u}}{\partial \psi} \right] + \frac{\beta C}{\bar{u} F} \tag{12}$$

Diffusion:

$$\frac{\partial C}{\partial \bar{z}} = \frac{(\beta C + 1)^2}{Re_{1,0} Sc_{1,0}} \frac{\partial}{\partial \psi} \left(\overline{Dr^2 u} \frac{\partial C}{\partial \psi} \right) \tag{13}$$

Because of the cylindrical geometry the $\bar{r}$ does not drop out of the equations as in the work of Pai, and a relation between ψ and $\bar{r}$ must be carried along with the transformed equations set. Since $\partial\psi/\partial\bar{z}$ is zero at $z = 0$ and very small elsewhere, it is neglected here; from equations (8) the following is obtained:

$$\int_0^{\psi} d\psi^* = \int_0^{\bar{r}} \bar{u}(\beta C + 1) \bar{r}^* \, d\bar{r}^* \tag{14a}$$

where $*$ denotes the dummy variable. This relation will be used for the initial conditions since they are expressed as functions of $\bar{r}$. During the integration where $\bar{r}$ is a dependent variable, the following is used:

$$\int_0^{\bar{r}} \bar{r}^* \, d\bar{r}^* = \int_0^{\psi} \frac{1}{\bar{u}(\beta C + 1)} d\psi^* \tag{14b}$$

The numerical integration is made with equations (12) to (14) and is described in appendix A.

As an aid in presenting the results, two terms are defined. The first term, the average axial velocity of inner-stream component at some axial station, is defined as

$$\bar{u}_{av,1} = \frac{\int_0^{\infty} \bar{u} C \bar{r} \, d\bar{r}}{\int_0^{\infty} C \bar{r} \, d\bar{r}}$$

The second term, the inner-fluid average density, is defined from continuity of the inner fluid. It represents the amount of inner fluid present in a cylindrical section of radius r_{max} and length L divided by the amount of inner-stream fluid that would have been present in the section had both streams been initially moving with the same velocity. The radius r_{max} is chosen large enough so that

there is no flow of inner-stream component out the sides of the cylinder. Since the pressure and temperature are constant, an average density at any axial station is simply

$$\bar{\rho}_{av} = \frac{1}{\bar{u}_{av}}$$

and the inner-fluid average density is defined as

$$\bar{\rho}_{av,L} = \frac{1}{L} \int_0^L \frac{d\bar{z}}{\bar{u}_{av}}$$

RESULTS AND DISCUSSION

The results obtained by this analysis are discussed in this section in terms of the potential core of the inner fluid. This term is used to mean the undisturbed flow inside the mixing region between the two coaxial streams. Neither nature nor the equations, however, allow for undisturbed flow in contact with disturbed flow. As soon as the outer fibers of the inner stream experience acceleration, all the inner fibers also accelerate (some only to an infinitesimal extent). It is necessary, for this reason, to legislate a potential core. This is done by considering all the inner fluid that has a velocity less than 1.05 times the initial inner-fluid velocity to lie in the potential core (see fig. 1).

The accuracy of the results of this analysis is tied in large part to the assumption that

$$\frac{\partial u}{\partial r} \gg \frac{\partial u}{\partial z}$$

and

$$\frac{\partial C}{\partial r} \gg \frac{\partial C}{\partial z}$$

This assumption is especially in doubt in the region close to the entrance. All the results presented here, however, are for this region between the entrance and the end of the potential core. To illustrate that the results are not obviously invalid, these derivatives are calculated for the case of largest density and velocity gradients along the z-direction at a radius of approximately 1 (fig. 2). This region along the boundary of the jets exhibits the largest values of the partial derivatives in both directions. It is seen from the curves that, while the value of the ratio $\frac{\partial C/\partial \bar{z}}{\partial C/\partial \bar{r}}$ starts at about 0.5, it drops to a value below 0.1 at $\bar{z} = 2$. The ratio of $\frac{\partial \bar{u}/\partial \bar{z}}{\partial \bar{u}/\partial \bar{r}}$ is seen to remain at a very low value for the

whole region of interest. Since the calculations are made with this assumption included, this proof of validity is not conclusive but is inferred from the small values of the ratios.

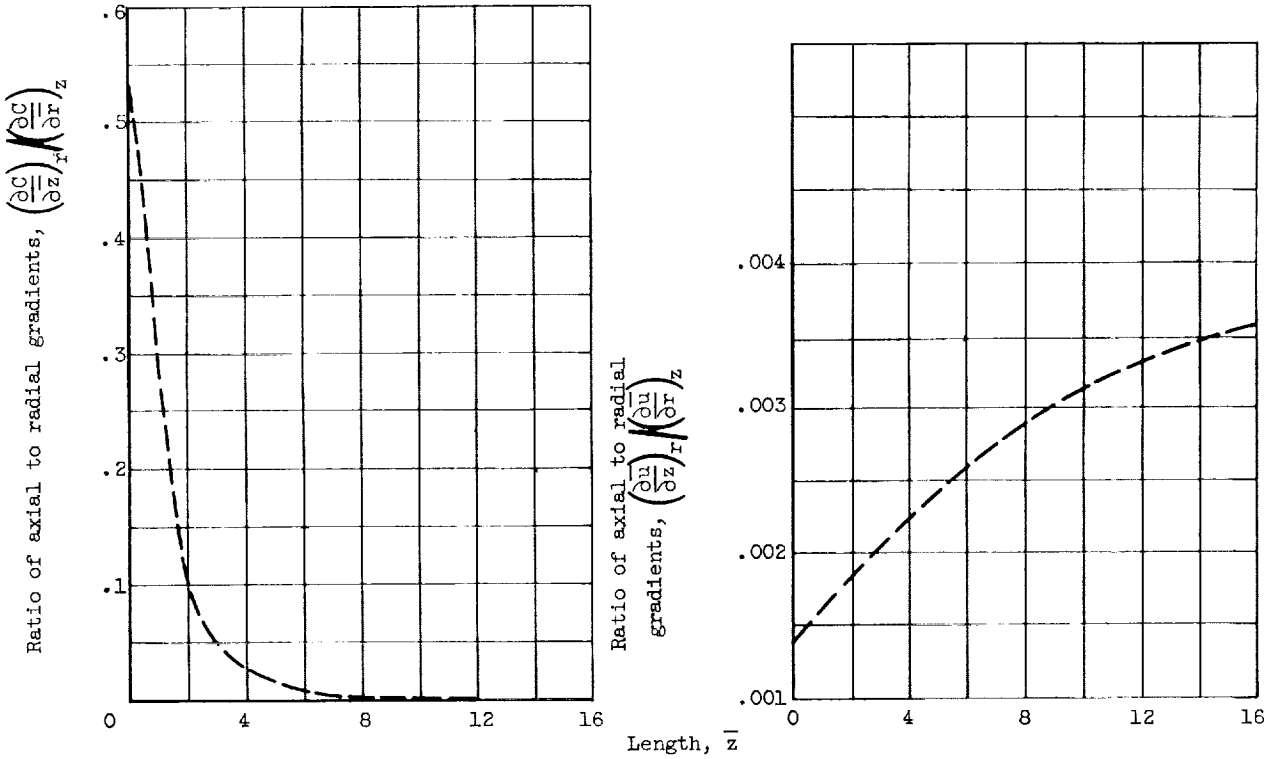

Figure 2. - Evaluation of validity of boundary-layer assumptions. Reynolds number, 1000; Schmidt number, 1; molecular volume ratio, 0.2; viscosity ratio, 0.2; velocity ratio of outer to inner streams, 100; density ratio of inner to outer streams, 100; Froude number, ∞.

It can be seen from the differential equations describing the flow phenomena that, when body forces are neglected, the Reynolds number of the inner stream at the initial conditions appears only as a constant factor in both equations (12) and (13) and does not appear at all in equations (14a) and (14b). The equations could have been solved in terms of $\bar{z}/Re_{1,0}$; then the Reynolds number would not have appeared at all in the equations. Hence, the Reynolds number has no effect on the velocity and concentration profiles or on the mixing in the absence of body forces as long as the flow is laminar. Changing the Reynolds number will only affect the axial location at which a profile exists and not the shape it takes. The data that appear here can be made to apply for any Reynolds number by manipulation of the $\bar{z}$-coordinate. The real effect of the Reynolds number is on the stability of the flow system with which this report is not concerned. For these reasons all the data that are presented here are for $Re_{1,0} = 1000$.

The main body of results presented here is for flat initial velocity and concentration profiles. Flat profiles were chosen for simplicity in calculation despite the fact that a singularity exists where the profiles meet. This flow would be more stable than flow with a velocity profile that was not monotonically increasing with radius, such as two parabolic profiles both reaching zero at $\bar{r} = 1$.

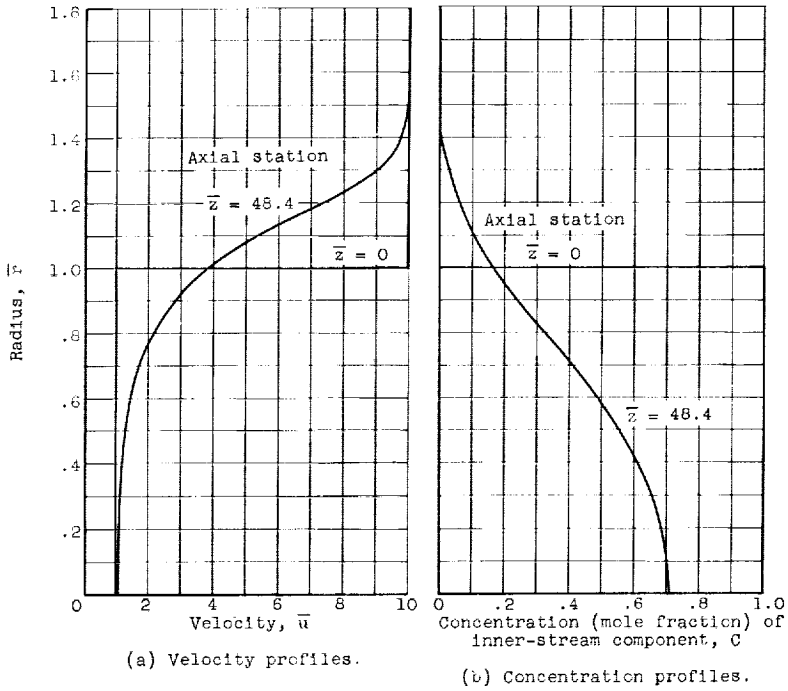

Figure 3. - Velocity and concentration profiles with flat initial profiles. Reynolds number, 1000; Schmidt number, 1; molecular volume ratio, 0.2; viscosity ratio, 0.2; velocity ratio of outer to inner streams, 10; density ratio of inner to outer streams, 10; Froude number, ∞.

Figure 3 shows typical velocity and concentration profiles that have flat initial profiles. The case illustrated has a velocity ratio of outer to inner streams of 10 and a density ratio of inner to outer streams of 10, both intermediate values in the range of values considered. The axial position of the profiles is at $\bar{z} = 48.4$, which as the profiles show is near the end of the potential core, since the center streamline has accelerated to a value of about 5 percent above the initial value. The velocity profile is a smooth curve, monotonically increasing in the increasing $\bar{r}$-direction. There is an inflection point in the curve that represents a potentially unstable flow condition. The concentration profile in figure 3(b) is a smooth monotonically decreasing curve and also exhibits an inflection point. It also should be noted that a comparison of figures 3(a) and (b) shows the momentum mixing region is larger than the concentration mixing region.

The end of the potential core is considered as that point at which the centerline velocity reaches 1.05 times the initial centerline velocity. The length of the potential core is a function of both the mass density function and the initial velocity ratio as shown in figure 4. It is seen that the potential core length increases with increasing β and decreasing $\overline{u}_2$ values. It is interesting to note that even for $\beta = 0$, which corresponds to fluids of the same density or the same fluid in each stream, and $\overline{u}_2 = 100$, the potential core extends for approximately 6 radii downstream. For $\beta = 50$ and $u_2 = 5$, the potential core extends for approximately 76 radii downstream. The end of the potential core corresponds to the point at which succeeding velocity profiles become similar and similarity solutions become valid, and therefore is an important result of this analysis.

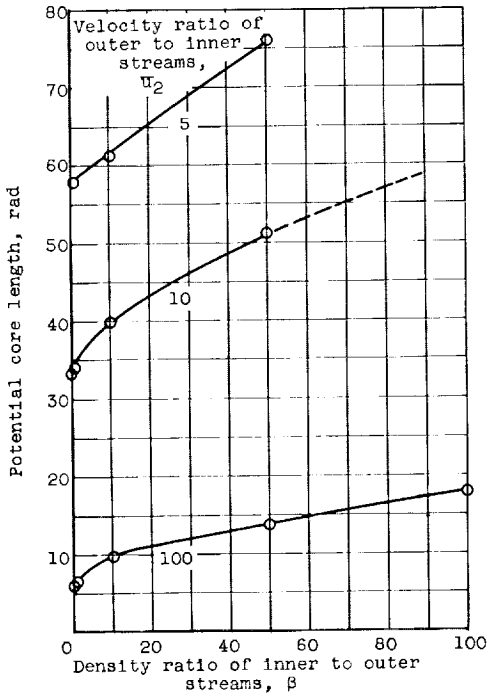

Figure 4. - Length of potential core as a function of density and initial velocity ratios. Reynolds number, 1000; Schmidt number, 1; molecular volume ratio, 0.2; viscosity ratio, 0.2; Froude number, ∞.

The axial velocity of the inner-stream fluid, averaged in the radial direction, at the end of the potential core is the subject of figure 5. The curves show that $\overline{u}_{av,1}$ increases as $\overline{u}_2$ increases and β decreases; however, the effect of β variation becomes very small at values of β greater than 20. The values for $\overline{u}_{av,1}$ at the end of the potential core, ranging from about 2 to 5

for the range of variables considered, indicates the acceleration of the inner fluid that takes place before a similarity solution becomes valid.

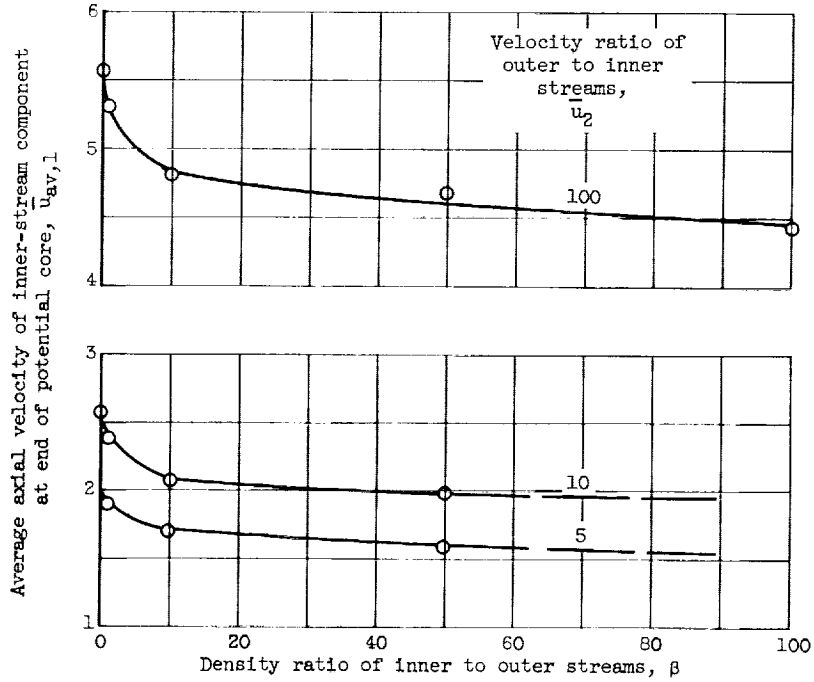

Figure 5. - Average axial velocity at end of potential core as a function of density ratio. Reynolds number, 1000; Schmidt number, 1; molecular volume ratio, 0.2; viscosity ratio, 0.2; Froude number, ∞.

Figure 6 shows the average density of inner-fluid component for the region between $\bar{z} = 0$ and $\bar{z} = 15$ as a function of the initial density. The sensitivity of inner-stream average density to changing β increases markedly for increasing values of $\bar{u}_2$. At a value of $\bar{u}_2 = 100$, the average density increases from about 0.15 to 0.40 as β varies from 0 to 100. This result has an interesting application to the gaseous, coaxial-flow, nuclear-reactor concept of reference 3. Values of $\bar{u}_2 = 100$, $\beta = 100$, and a final $\bar{z} = 15$ comply with one of the cases of reference 3, and the resultant value of the average density of 0.40 is very encouraging for this concept.

The effect of a body force acting along the flow axis in the same direction as the flow is shown in figure 7. The Froude number contains the acceleration term due to the body force in the denominator; hence, as the Froude number approaches infinity, the body force approaches zero. Here, again, the potential core is made up of fluid moving at or near the initial inner-stream velocity so that the potential core length approaches zero as the Froude number becomes small. This plot of potential core length as a function of Froude number for a given set of parameters illustrates that, for Froude numbers of the order of 10^2

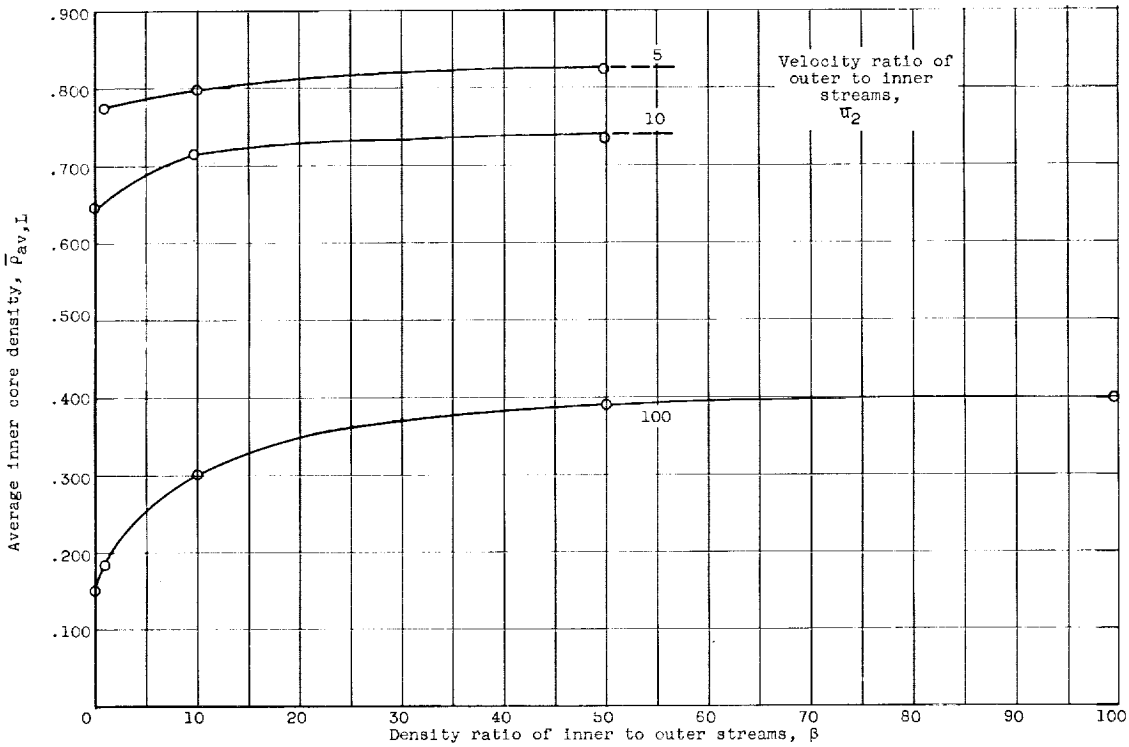

Figure 6. - Inner-fluid average density as a function of density ratio. Reynolds number, 1000; Schmidt number, 1; molecular volume ratio, 0.2; viscosity ratio, 0.2; Froude number, ∞.

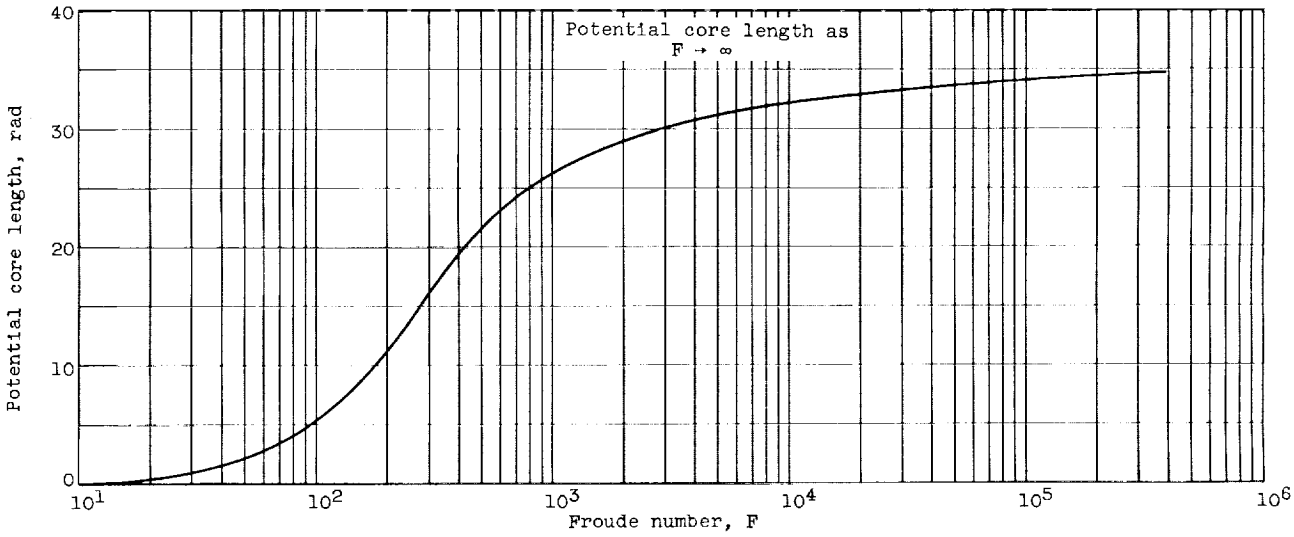

Figure 7. - Effect of Froude number on potential core length. Reynolds number, 1000; Schmidt number, 1; molecular volume ratio, 0.2; viscosity ratio, 0.2; velocity ratio of outer to inner streams, 10; density ratio of inner to outer streams, 10.

or less, the mass and momentum transfer become second-order effects compared to the acceleration caused by the force field. The case shown is for $\beta = 10$, which is representative of cases with high β. This is so because the body force term is of the form $\beta C/[F(\beta C + 1)]$ or, on rearranging, $1\Big/\left[F\left(1 + \frac{1}{\beta C}\right)\right]$. As β becomes very large, this term can be approximated as $1/F$ inside the potential core. When β is small, the effect is small; and at $\beta = 0$ the body forces have no effect.

Figure 8 illustrates the effect of physical property variation. The effect of Schmidt number variation is shown in figure 8(a). For a change in Schmidt number by a factor of 10, the length of the potential core and the $\overline{u}_{av,1}$ at the end of the potential core only change by approximately a factor of 2. Figure 8(b) shows the effect of changing the viscosity ratio. Hence, for a tenfold change in $\overline{\mu}_2$ the potential core length changes by approximately a factor of 3, but the $\overline{u}_{av,1}$ changes only by about 1.2. Finally, the effect of changing the molecular volume ratio $\overline{V}_2$ of the two components is shown in figure 8(c). Once again, for a tenfold change in $\overline{V}_2$ the potential core length changes by only a factor of somewhat less than 2, and the $\overline{u}_{av}$ at the end of the potential core changes by only 10 percent or so.

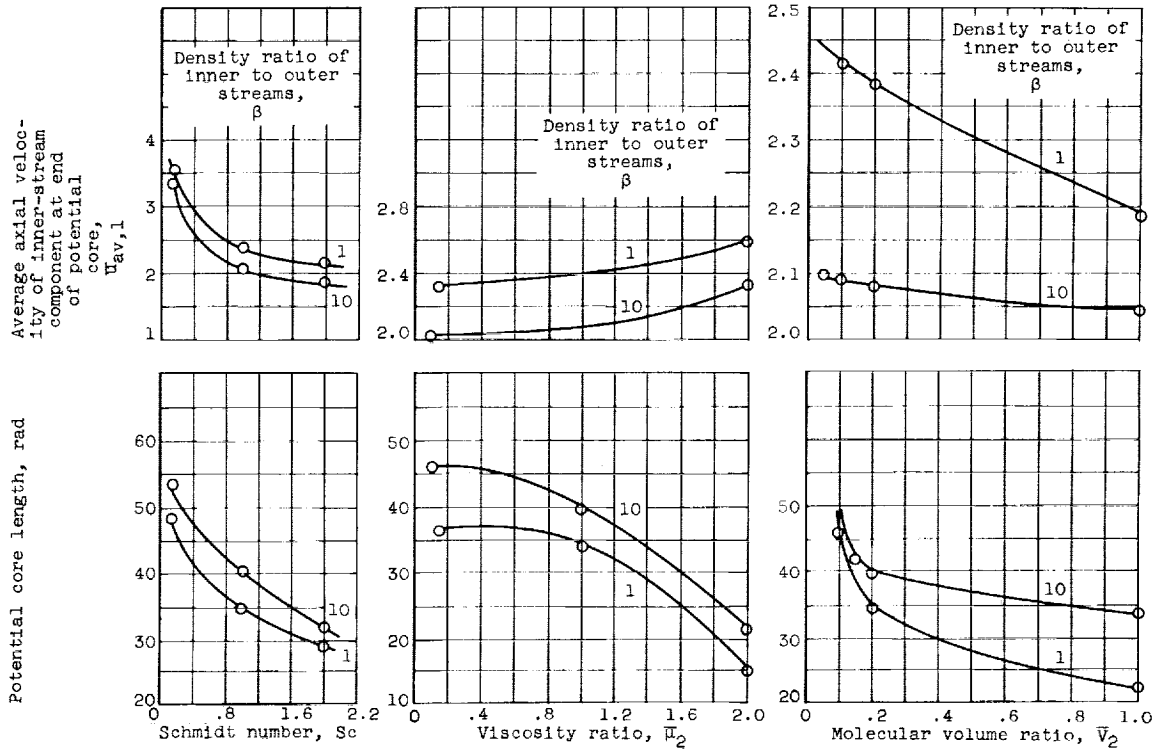

(a) Schmidt number. Molecular volume ratio, 0.2; viscosity ratio, 0.2.

(b) Viscosity ratio. Schmidt number, 1; molecular volume ratio, 0.2.

(c) Molecular volume ratio. Schmidt number, 1; viscosity ratio, 0.2.

Figure 8. - Effect of physical property variations. Reynolds number, 1000; velocity ratio of outer to inner streams, 10; Froude number, ∞.

These last curves show that the choice of dimensionless groups made in this approach was quite fortunate and that results obtained from it should be valuable even though the physical properties used in the calculation were only approximate values.

Figure 9 shows the velocity and concentration profiles for a case with parabolic inlet velocity profiles, which are plotted with the same values of input parameters. The very slow-moving region at $\bar{r} = 1$ slows down the flow around it and prevents early acceleration of the inner stream, which would provide for much longer potential core lengths than were found for the slug-flow cases. This type of nonmonotonic velocity profile, however, is extremely unstable hydrodynamically and is included here only as a point of interest.

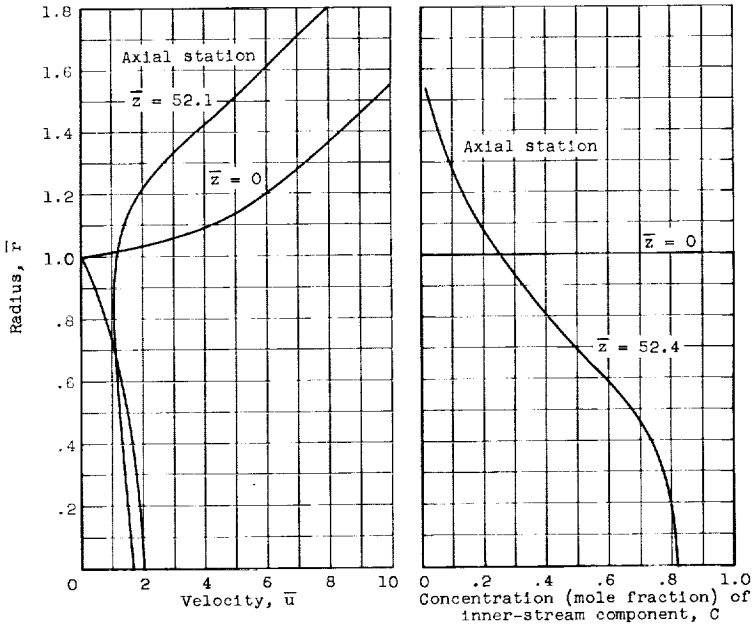

Figure 9. - Velocity and concentration profiles with parabolic inlet velocity profiles. Reynolds number, 1000; Schmidt number, 1; viscosity ratio, 0.2; velocity ratio of outer to inner streams, 10; density ratio of inner to outer streams, 10; Froude number, ∞.

SUMMARY OF RESULTS

In this research study, an analysis for the isothermal, laminar coaxial flow of two fluids is presented. The analysis is based on certain assumptions, mainly, the boundary-layer simplifications and constant pressure in the flow field. The analysis resulted in an equation set, which was solved numerically. Typical results yielded by this analysis are summarized under the two categories of general and specific results. The general results are as follows:

1. The velocity and concentration profiles are smooth curves, and both contain inflection points. Velocity increases monotonically and concentration of

inner-stream component decreases monotonically out from a radius or stream function value of zero.

2. The potential core length increases with increasing density ratio of inner- to outer-stream components; it decreases with increasing velocity ratio of outer to inner streams.

3. Increasing axial acceleration forces in the direction of flow, as measured by the Froude number, shortens the length of the potential core.

4. Changing the initial velocity profile from a flat to a parabolic form increases the potential core length markedly for this analysis.

For the following parametric values: Reynolds number, 1000; Schmidt number, 1; molecular volume ratio, 0.2; viscosity ratio, 0.2; the following specific results were found:

1. For fluids of the same density and a velocity ratio of outer to inner streams of 100, the potential core length remains approximately 6 radii.

2. The average velocity of the inner-stream component at the end of the potential core increases as the velocity ratio of outer to inner streams increases and the density ratio of inner to outer streams decreases. For values of density ratio of inner to outer streams greater than 20, the effect of varying the density ratio is small.

3. For a velocity ratio of outer to inner streams of 100, the average inner-stream density for the region 15 radii long starting at the initial face increases approximately threefold as the density ratio of inner to outer streams varies from 0 to 100.

4. For a velocity ratio of outer to inner streams of 10, a density ratio of inner to outer streams of 10, and Froude numbers of 10^2 or less, the mass and momentum transfer become second-order effects compared to the acceleration caused by the force field.

5. For a velocity ratio of outer to inner streams of 10 and a density ratio of inner to outer streams of 10, changing the Schmidt number from a value of 2 to a value of 0.2 increases the potential core length by a factor of 2; changing the viscosity ratio from 0.2 to 2 decreases the potential core length by a factor of 3; and changing the molecular volume ratio from 0.2 to 1 decreases the potential core length by a factor of approximately 2.

Lewis Research Center
National Aeronautics and Space Administration
Cleveland, Ohio, October 1, 1962

APPENDIX A

NUMERICAL INTEGRATION

The differential equations, which define the physical system, are:

$$\frac{\partial u}{\partial z} = \frac{\beta + 1}{Re} \frac{\partial}{\partial \psi} \left[\mu r^2 u(\beta C + 1) \frac{\partial u}{\partial \psi} \right] + \frac{\beta C}{F(\beta C + 1)} \tag{A1}$$

$$\frac{\partial C}{\partial z} = \frac{(\beta C + 1)^2}{Re\ Sc} \frac{\partial}{\partial \psi} \left(Dr^2 u \frac{\partial C}{\partial \psi} \right) \tag{A2}$$

$$r^2 = 2 \int_0^{\psi} \frac{d\psi^*}{u(\beta C + 1)} \tag{A3}$$

$$\mu = \frac{\beta C + 1}{(\beta + 1)C + \frac{1 - C}{\mu_2}} \tag{A4}$$

These equations are integrated numerically to obtain the solution of each function ($u = u(\psi,z)$, $C = C(\psi,z)$, $r = r(\psi,z)$, and $\mu = \mu(\psi,z)$) in the semi-infinite strip $R:\{0 \leq \psi \leq \psi_{max},\ z \geq 0\}$.

The description of the system at $z = 0$ is given by the following relations:

$$u(\psi,0) = u(r) \tag{A5}$$

$$C(\psi,0) = C(r) \tag{A6}$$

$$\psi(r) = \int_0^r u(r^*)\ \beta C(r^*) + 1\ r^*\ dr^* \tag{A7}$$

Also, at $z = 0$,

$$\frac{\partial \psi}{\partial z} = 0 \tag{A8}$$

Now if the flat initial profiles, $u(r)$ and $C(r)$, are defined as functions of the radius by:

$$u(r) = 1,\ C(r) = 1 \qquad (0 \leq r \leq 1) \tag{A9}$$

$$u(r) = u_2,\ C(r) = 0 \qquad (1 < r \leq r_{max}) \tag{A10}$$

then substituting the values of $u(r)$ and $C(r)$ given in equations (A9) and (A10) into equation (A7) produces the relations:

$$u(\psi,0) = 1,\ C(\psi,0) = 1 \qquad \left(0 \le \psi \le \frac{\beta + 1}{2}\right) \tag{A11}$$

$$u(\psi,0) = u_2,\ C(\psi,0) = 0 \qquad \left(\frac{\beta + 1}{2} < \psi \le \psi_{max}\right) \tag{A12}$$

A substitution of the relations derived in equations (A11) and (A12) into equation (A7) yields at $z = 0$

$$r^2(\psi) = \frac{2\psi}{\beta + 1} \qquad (0 \le r \le 1) \tag{A13}$$

and

$$r^2(\psi) = \left[\left(\psi - \frac{\beta + 1}{2}\right)\frac{2}{u_2}\right] + 1 \qquad (1 < r \le r_{max}) \tag{A14}$$

The solution of the given system is obtained by using finite difference methods. By dividing the semi-infinite strip $R:\{0 \le \psi \le \psi_{max},\ z \ge 0\}$ into a number of rectangles, a grid or mesh is constructed of dimension mxn. Hence the notation, $R_{i,j}$ would denote the i^{th}, j^{th} point on the mesh. If $u(\psi_i,z_j)$ is defined as the functional value of $u(\psi,z)$ associated with the mesh point $R_{i,j}$, the formal derivative approximations may be described as

$$u_\psi(\psi_i,z_j + \theta\,\Delta z) \approx \frac{1}{2\,\Delta\psi}\left[u(\psi_{i+1},z_{j+\theta}) - u(\psi_{i-1},z_{j+\theta})\right] \tag{A15}$$

$$u_{\psi\psi}(\psi_i,z_j + \theta\,\Delta z) \approx \frac{1}{(\Delta\psi)^2}\left[u(\psi_{i+1},z_{j+\theta}) - 2u(\psi_i,z_{j+\theta}) + u(\psi_{i-1},z_{j+\theta})\right] \tag{A16}$$

$$u_z(\psi_i,z_j + \theta\,\Delta z) \approx \frac{1}{\Delta z}\left[u(\psi_i,z_{j+1}) - u(\psi_i,z_j)\right] \tag{A17}$$

where $0 \le \theta \le 1$.

Applying approximations (A15) to (A17) to equations (A1) to (A4) (with $\theta = 0$) results in:

$$u(\psi_i,z_{j+1}) = \frac{\Delta z}{2\,\Delta\psi}\frac{\beta + 1}{Re}\left[G(\psi_{i+1},z_j) - G(\psi_{i-1},z_j)\right] + u(\psi_i,z_j) + \frac{\beta C(\psi_i,z_j)}{F\left[\beta C(\psi_i,z_j) + 1\right]} \tag{A18}$$

where

$$\left.\begin{aligned} G(\psi_i,z_j) &= \mu(\psi_i,z_j)r^2(\psi_i,z_j)u(\psi_i,z_j)\left[\beta C(\psi_i,z_j) + 1\right] \\ &\qquad \times \frac{1}{2\,\Delta\psi}\left[u(\psi_{i+1},z_j) - u(\psi_{i-1},z_j)\right] \\ C(\psi_i,z_{j+1}) &= \frac{\Delta z}{2\,\Delta\psi}\,\frac{\left[\beta C(\psi_i,z_j) + 1\right]^2}{Re\ Sc}\left[H(\psi_{i+1},z_j) - H(\psi_{i-1},z_i)\right] \end{aligned}\right\} \qquad (A19)$$

where

$$\left.\begin{aligned} H(\psi_i,z_j) &= Dr^2(\psi_i,z_j)u(\psi_i,z_j)\,\frac{1}{2\,\Delta\psi}\left[C(\psi_{i+1},z_j) - C(\psi_{i-1},z_j)\right] \\ r^2(\psi_i,z_{j+1}) &= \int_0^{\psi_{max}} \frac{d\psi}{u(\psi,z_{j+1})\left[\beta C(\psi_i,z_{j+1}) + 1\right]} \end{aligned}\right\} \qquad (A20)$$

and

$$\mu(\psi_i,z_{j+1}) = \frac{\beta C(\psi_i,z_{j+1}) + 1}{(\beta + 1)C(\psi_i,z_{j+1}) + \dfrac{1 - C(\psi_i,z_{j+1})}{\mu_2}} \qquad (A21)$$

If equations (A11) to (A14) are used, the description of the system at $z = 0$ becomes

$$\left.\begin{aligned} u(\psi_i,0) &= 1, \qquad C(\psi_i,0) = 1 \qquad \left(0 \le \psi_i \le \frac{\beta + 1}{2}\right) \\ u(\psi_i,0) &= u_2, \qquad C(\psi_i,0) = 0 \qquad \left(\frac{\beta + 1}{2} < \psi_i \le \psi_{max}\right) \end{aligned}\right\} \qquad (A22)$$

$$\left.\begin{aligned} r^2(\psi_i,0) &= \frac{2\psi_i}{\beta + 1} \qquad \left[0 \le r(\psi_i) \le 1\right] \\ r^2(\psi_i,0) &= \frac{\left(\psi_i - \dfrac{\beta + 1}{2}\right)2}{u_2 + 1} \qquad \left[1 < r(\psi_i) \le r_{max}\right] \end{aligned}\right\} \qquad (A23)$$

Hence, given values of β, Re, Sc, **F**, V_2, μ_2, and ψ_{max}, numerical solutions for $u(\psi_i,z_j)$, $C(\psi_i,z_j)$, $r(\psi_i,z_j)$, and $\mu(\psi_i,z_j)$ can be obtained for any point $R_{i,j}$

on the strip R, starting at $z = 0$. The stability of the solution is a function of the mesh ratio $\lambda = \Delta z/(\Delta\psi)^2$. The following method for obtaining a stable solution is obtained from reference 6:

Let $\partial u/\partial z = \varphi(\psi, z, u, u_\psi, u_{\psi\psi})$ and define parameters a and b such that

$$\frac{\partial \varphi}{\partial u_{\psi\psi}} \geq a > 0 \tag{A24}$$

and

$$\left|\frac{\partial \varphi}{\partial u}\right| + \left|\frac{\partial \varphi}{\partial u_\psi}\right| + \left|\frac{\partial \varphi}{\partial u_{\psi\psi}}\right| \leq b \tag{A25}$$

Now if $\Delta\psi$ is chosen such that

$$\Delta\psi \leq \frac{2a}{b} \tag{A26}$$

then a λ that will yield a stable solution can be computed from

$$0 \leq \lambda \leq \frac{1 - b\,\Delta z}{2b} \tag{A27}$$

If a $\Delta\psi$ is chosen such that relation (A26) is satisfied, then Δz can be computed from:

$$\lambda = \frac{\Delta z}{(\Delta\psi)^2}$$

and

$$\lambda \leq \frac{1 - b\,\Delta z}{2b}$$

or

$$\Delta z \leq \frac{(\Delta\psi)^2}{b\left[2 + (\Delta\psi)^2\right]} \tag{A28}$$

Application of the aforementioned theorem to equation (A1) with the assumption that C, μ, and r are known functions of ψ and z results in

$$\frac{\partial u}{\partial z} = \frac{\beta + 1}{Re}\frac{\partial}{\partial \psi}\left[\mu r^2 u(\beta C + 1)\frac{\partial u}{\partial \psi}\right] = \varphi_1(\psi, z, u, u_\psi, u_{\psi\psi})$$

Hence,

$$\frac{\partial \varphi_1}{\partial u} = \frac{\beta + 1}{Re}\left[r^2(\beta C + 1)\frac{\partial u}{\partial \psi}\frac{\partial \mu}{\partial \psi} + 2r\mu(\beta C + 1)\frac{\partial r}{\partial \psi}\frac{\partial u}{\partial \psi} + \mu r^2\beta\frac{\partial C}{\partial \psi}\frac{\partial u}{\partial \psi} + \mu r^2(\beta C + 1)\frac{\partial^2 u}{\partial \psi^2}\right]$$

$$\frac{\partial \varphi_1}{\partial u_\psi} = \frac{\beta + 1}{Re}\left[r^2 u(\beta C + 1)\frac{\partial u}{\partial \psi} + 2r\mu u(\beta C + 1)\frac{\partial r}{\partial \psi} + 2\mu r^2(\beta C + 1)\frac{\partial u}{\partial \psi} + \mu r^2 u\beta\frac{\partial C}{\partial \psi}\right]$$

$$\frac{\partial \varphi_1}{\partial u_{\psi\psi}} = \frac{\beta + 1}{Re}\mu r^2 u(\beta C + 1)$$

and

$$a_1 = \frac{\partial \varphi_1}{\partial u_{\psi\psi}}$$

$$b_1 = \left|\frac{\partial \varphi_1}{\partial u}\right| + \left|\frac{\partial \varphi_1}{\partial u_\psi}\right| + \left|\frac{\partial \varphi_1}{\partial u_{\psi\psi}}\right|$$

and thus, in order to obtain a stable solution,

$$\Delta\psi = \frac{2a_1}{b_1}$$

$$\Delta z = \frac{(\Delta\psi)^2}{b_1\left[2 + (\Delta\psi)^2\right]} \tag{A29}$$

It was found that the value of $\Delta\psi$ that would satisfy inequality (A26) could be established from initial conditions; hence it was necessary to compute only values of Δz that varied directly with z.

Large values of u_2 and β seriously limited the accuracy of the solution because of truncation errors; hence the following less sophisticated method was employed for these extreme cases. To avoid these errors, it is required that the functional value of $C(\psi_i, z_{j+1})$ vary less than some fixed percentage of $C(\psi_i, z_j)$. Let K be a number such that $0 < |K| \leq 1$; the change of $C(\psi_i, z_{j+1})$ could be described as

$$C(\psi_i, z_{j+1}) = C(\psi_i, z_j)(1 + K) \tag{A30}$$

From the finite difference approximation, equation (A30) becomes

$$\frac{\partial C(\psi_i, z_j)}{\partial z} \approx \frac{C(\psi_i, z_{j+1}) - C(\psi_i, z_j)}{\Delta z} \tag{A31}$$

Substitution of equation (A29) into (A30) yields

$$\frac{\partial C(\psi_i, z_j)}{\partial z} \approx \frac{KC(\psi_i, z_j)}{\Delta z} \tag{A32}$$

or, in terms of Δz, relation (A32) can be written:

$$(\Delta z)_i = \left| \frac{KC(\psi_i, z_j)}{\frac{\partial C(\psi_i, z_j)}{\partial z}} \right|$$

Hence, the Δz to be used at each j^{th} interval is

$$\Delta z = \min\left[(\Delta z)_i\right] \tag{A33}$$

The Δz computed in this manner is approximately one order of magnitude less than the Δz calculated by equation (A29). Thus, if a $\Delta\psi$ is chosen that satisfies relation (A26), stability is assured.

APPENDIX B

LENNARD-JONES POTENTIAL DIFFUSIVITY

The value of $\overline{D}$, the dimensionless diffusivity equal to D_{12}/D_{11}, can also be derived from the Lennard-Jones potential argument. The method is as follows:

$$\frac{D_{12}}{D_{11}} = \frac{\dfrac{\sqrt{\dfrac{T^3(m_1 + m_2)}{2m_1m_2}}}{P\sigma_{12}^2\Omega D_{12}\left(\dfrac{KT}{\epsilon_{12}}\right)}}{\dfrac{\sqrt{\dfrac{T^3}{m_1}}}{P\sigma_1\Omega D_{11}\left(\dfrac{KT}{\epsilon_{11}}\right)}}$$

(ref. 7) or

$$\frac{D_{12}}{D_{11}} = \sqrt{2(\beta + 2)}\left[2\sqrt{\frac{\epsilon_2}{\epsilon_1}}\ \frac{\dfrac{\Omega D_1}{\Omega D_{12}}}{\left(1 + \dfrac{\sigma_2}{\sigma_1}\right)^2}\right]$$

Then the term

$$\frac{1}{1 + \overline{V}_2^{1/3}}$$

from the Gilliland equation corresponds to

$$2\sqrt{\frac{\epsilon_2}{\epsilon_1}}\ \frac{\dfrac{\Omega D_1}{\Omega D_{12}}}{\left(1 + \dfrac{\sigma_2}{\sigma_1}\right)^2}$$

from the Lennard-Jones potential argument. The value of $\overline{D}$ then is constant when evaluated by either method.

REFERENCES

1. Pai, Shih-I: Fluid Dynamics of Jets. D. Van Nostrand Co., Inc., 1954.

2. Torda, T. P., and Stillwell, H. D.: Analytical and Experimental Investigations of Incompressible and Compressible Mixing of Streams and Jets. TR 55-347, WADC, Mar. 1956.

3. Weinstein, Herbert, and Ragsdale, Robert G.: A Coaxial Flow Reactor - A Gaseous Nuclear-Rocket Concept. Preprint 1518-60, Am. Rocket Soc., Inc., 1960.

4. Grey, Jerry: Heat Transfer from an Ionized Gas to a Gaseous Coolant. Rep. 437-A, Aero. Eng. Lab., Princeton Univ., July 1959.

5. Bird, R. Byron, Stewart, Warren E., and Lightfoot, Edwin C.: Notes on Transport Phenomena. John Wiley & Sons, Inc., 1958.

6. Douglas, Jim, Jr.: On the Numerical Integration of Quasi-Linear Parabolic Differential Equations. Pacific Jour. Math, vol. 6, 1956, pp. 35-42.

7. Hirschfelder, Joseph O., Curtiss, Charles F., and Bird, R. Byron: Molecular Theory of Gases and Liquids. John Wiley & Sons, Inc., 1954.